Quantum-brachistochrone approach to the conversion from *W* to Greenberger-Horne-Zeilinger states for Rydberg-atom qubits

Julian K. Nauth and Vladimir M. Stojanović

Institut für Angewandte Physik, Technical University of Darmstadt, D-64289 Darmstadt, Germany

Using the quantum-brachistochrone formalism, we address the problem of finding the fastest possible (time-optimal) deterministic conversion between *W* and Greenberger-Horne-Zeilinger (GHZ) states in a system of three identical and equidistant neutral atoms that are acted upon by four external laser pulses. Assuming that all four pulses are close to being resonant with the same internal (atomic) transition—the one between the atomic ground state and a high-lying Rydberg state—each atom can be treated as an effective two-level system (*gr*-type qubit). Starting from an effective system Hamiltonian, which is valid in the Rydberg-blockade regime and defined on a four-state manifold, we derive the quantum-brachistochrone equations pertaining to the fastest possible *W*-to-GHZ state conversion. By numerically solving these equations, we determine the time-dependent Rabi frequencies of external laser pulses that correspond to the time-optimal state conversion. In particular, we show that the shortest possible *W*-to-GHZ state-conversion time is given by $T_{\mathrm{QB}} = 6.8\,\hbar/E$, where E is the total laser-pulse energy used, this last time being significantly shorter than the state-conversion times previously found using a dynamical-symmetry-based approach [$T_{\mathrm{DS}} = (1.33 - 1.66)\,T_{\mathrm{QB}}$].

I. INTRODUCTION

The availability of fast, accurate protocols for the preparation of highly entangled quantum states is one of the crucial prerequisites for the adoption of next-generation quantum technologies [1]. In particular, maximally-entangled multiqubit states of *W*- [2] and Greenberger-Horne-Zeilinger (GHZ) [3] type are of both conceptual and practical importance in the realm of quantum-information processing (QIP) [4]. Owing to their already proven usefulness in QIP [5,6], a large number of schemes for the preparation of *W* [7–15] and GHZ states [16–24] in various physical platforms have been proposed in recent years. Among those platforms, one of the most promising ones from the standpoint of large-scale quantum computing and analog quantum simulation is based on ensembles of neutral atoms in Rydberg states [25–28]. Recent years have also seen growing general interest in quantum-state engineering in systems of this type [23,29–37].

Apart from various schemes for the efficient preparation of *W* or GHZ states, which usually entail product states as their starting point [32], the interconversion between those two maximally entangled states constitutes another relevant problem of quantum-state engineering. What makes the idea of interconversion between the two states— which, for example, in the three-qubit case represent the only two inequivalent classes of genuine tripartite entanglement [2] — particularly appealing is the apparent dissimiliarity as far as the character of entanglement in the two states is concerned [38]. For instance, three-qubit GHZ state has maximal distributed (essential three-way) entanglement, while pairwise bipartite entanglements all vanish [39]. On the other hand, for its *W*

counterpart the essential three-way entanglement vanishes, while it has strong pairwise entanglements [40].

The pioneering attempt of carrying out the *W*-to-GHZ state conversion pertained to a photonic system and its character was probabilistic [41]. Following this initial investigation, another work with photons was reported [42], as well as a study devoted to a spin system [43]. In the realm of neutral-atom systems, irreversible conversions of a *W* state into a GHZ state were proposed [44,45], followed by two proposals for the deterministic conversion between the two states in a laser-controlled system of three equidistant *gr*-type Rydberg-atom qubits [33,37]. The first among those proposals [33] utilized the method of shortcuts to adiabaticity, more precisely an inverse-engineering approach based on a Lewis-Riesenfeld-type dynamical invariant. The second one [37] — advanced by one of us and collaborators — was based on a Lie-algebraic approach that, under the assumption of real-valued Rabi frequencies of external laser pulses, explicitly takes into account the underlying dynamical symmetry $su(2) \oplus su(2) \cong so(4)$ of the effective system Hamiltonian defined on a manifold of four states (a basis of the permutation-symmetric subspace of the three-qubit Hilbert space). Importantly, the latter approach was shown to outperform the former in the sense of allowing the envisioned state conversion to be carried out up to five times faster (for the same total laser-pulse energy used), with a much simpler time dependence of the corresponding Rabi frequencies of laser pulses used.

In this paper, aiming to find the time-optimal *W*-to-GHZ state conversion in the same physical setting as Refs. [33,37], i.e. for a system of three equidistant neutral atoms interacting through van der Waals-type interaction, we employ the quantum-brachistochrone (QB) formalism [46]. Inspired in

part by the time-honored brachistochrone problem in classical mechanics [47], this formalism was proposed by Carlini and coworkers with the aim of finding the fastest possible quantum evolution from a given initial to a desired final state [46]. It allows one to find time-optimal control protocols under the assumption that the system Hamiltonian has a bounded norm, being at the same time restricted to a subspace of Hermitian operators. Subsequently, the formalism was generalized so as to treat the problem of finding time-optimal unitary operations [48] and utilized for solving realistic gate-optimization problems [49]. It has also led to important insights into a wide range of other problems of quantum physics [50–52].

Using the QB formalism we derive a system of first-order ordinary differential equations connecting the physical variables of interest in the problem at hand (namely, three time-dependent Rabi frequencies of external laser pulses, the corresponding auxiliary variables that have the nature of Lagrange multipliers, and the projections of the relevant quantum state of the system on the four relevant basis states). We then solve the two-point boundary value problem that corresponds to the shortest possible W-to-GHZ state conversion numerically using the *shooting method* (see, e.g., Ref. [53]), where the computational burden involved is substantially alleviated by means of an unconventional, problem-specific parametrization of the initial conditions. In this manner, we demonstrate that the time-optimal W-to-GHZ state conversion is 25–40 % faster than the protocol based on the dynamical-symmetry approach of Ref. [37] that requires real-valued Rabi frequencies. We also show that the three complex-valued (time-dependent) Rabi frequencies corresponding to the shortest-possible state conversion have time-independent phases. Moreover, we show that two of those phases can be chosen freely, with only the third one being constrained by the chosen values of the first two.

The remainder of this paper is organized as follows. In Sec. II we introduce the Rydberg-atom system under consideration and state its previously derived effective Hamiltonian. In Sec. III the QB equations governing the time-optimal conversion of an initial W state into its GHZ counterpart in the Rydberg-atom system under consideration are derived, followed by a specific parametrization of their initial conditions that facilitates their subsequent numerical solution. The numerical solution of the QB equations is also discussed. In Sec. IV we present and discuss the obtained results for the time-dependent Rabi frequencies of external laser pulses that correspond to the time-optimal state conversion. We also compare the obtained minimal state-conversion time with the corresponding times found in Refs. [33] and [37]. Finally, we demonstrate the robustness of our state-conversion scheme to deviations from the obtained optimal time-dependent Rabi frequencies. Before closing, we summarize the paper and underscore our main conclusions in Sec. V. The essential details of the method employed to numerically solve the QB equations are briefly reviewed in the Appendix.

II. SYSTEM AND ITS EFFECTIVE HAMILTONIAN

In what follows, we consider a system of three identical and equidistant neutral atoms, e.g., of ^{87}Rb [for an illustration, see Fig. 1]. All three atoms are subject to the same four external
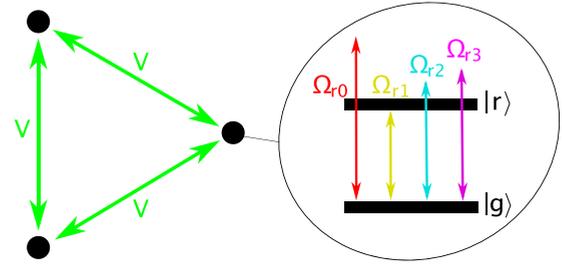
FIG. 1. Schematic of the system under consideration: Three identical and equidistant neutral atoms with the ground state $|g\rangle$ and a high-lying Rydberg state $|r\rangle$ (gr-type qubits) are acted upon by four external laser pulses, all close to being resonant with the transition between the states $|g\rangle$ and $|r\rangle$. $\hbar V$ is the magnitude of the vdW interaction.

laser pulses, whose respective Rabi frequencies are denoted by Ω_{r0}, Ω_{r1}, Ω_{r2}, and Ω_{r3}. It is hereafter assumed that the Rabi frequencies Ω_{r1}, Ω_{r2}, and Ω_{r3} are time dependent, while Ω_{r0} is time independent and envisioned to induce quadratic Stark shifts.

The four laser pulses are assumed to be close to the resonance with the same internal atomic transition, the one between the electronic ground state $|g\rangle$ and a highly-excited Rydberg state $|r\rangle$. Consequently, each atom can be treated as an effective two-level system; a gr-type Rydberg-atom qubit [27] where the states $|g\rangle$ and $|r\rangle$ play the role of logical $|0\rangle$ and $|1\rangle$ qubit states, respectively. The typical energy splitting of such qubits in frequency units is in the range $900 - 1500$ THz (the actual energy splitting depends on the choice of atomic species and Rydberg states used), thus their manipulation requires either an ultraviolet laser or a combination of visible and infrared lasers in a ladder configuration.

The Hamiltonian of the coupled atom-field system under consideration in the interaction picture is given by

$$H_{\mathrm{I}}(t)/\hbar = \sum_{s=1}^{3} \sum_{n=0}^{3} \Omega_{rn}(t) e^{-i(\delta_n + \Delta_n)t} |r\rangle_{ss}\langle g| + \mathrm{H.c.}$$
$$+ \sum_{s<s'} V |rr\rangle_{ss'}\langle rr|. \qquad (1)$$

The first term describes the interaction between each of the three atoms (indexed by $s, s' = 1, 2, 3$) and the four laser fields characterized by the Rabi frequencies Ω_{rn} ($n = 0, \ldots, 3$). The second one corresponds to the van der Waals (vdW) atom-atom interaction with the pairwise interaction energy $\hbar V$. The detunings of the four laser pulses from the relevant internal ($g - r$) transition are split into two parts δ_n and Δ_n ($n = 0, 1, 2, 3$), in keeping with Ref. [33].

As demonstrated in Ref. [33], through an appropriate choice of the detunings δ_n and Δ_n and under several conditions on other relevant parameters (interaction strength, laser-pulse duration, etc.) [37], the full system Hamiltonian of Eq. (1) can be reduced via perturbation theory to an effective one defined on a four-state manifold. The relevant four three-qubit states are the three-atom ground state $|ggg\rangle$, the W state

$$|W\rangle = \frac{1}{\sqrt{3}} (|rgg\rangle + |grg\rangle + |ggr\rangle), \qquad (2)$$
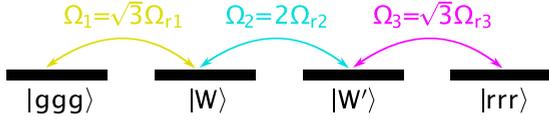
FIG. 2. Pictorial illustration of the effective system Hamiltonian $H(t)$ defined on a manifold of four states, where only pairs of adjacent states have nonzero coupling [cf. Eq. (4)].

the two-excitation Dicke state

$$|W'\rangle = \frac{1}{\sqrt{3}}\left(|rrg\rangle + |grr\rangle + |rgr\rangle\right), \tag{3}$$

and the state $|rrr\rangle$ with all three atoms occupying the Rydberg state.

The effective Hamiltonian is given by [33]

$$\begin{aligned}
H(t)/\hbar &= \Omega_1(t)|ggg\rangle\langle W| + \Omega_2(t)|W\rangle\langle W'| \\
&\quad + \Omega_3(t)|W'\rangle\langle rrr| + \text{H.c.,}
\end{aligned} \tag{4}$$

where $\Omega_1(t) \equiv \sqrt{3}\,\Omega_{r1}(t)$, $\Omega_2(t) \equiv 2\,\Omega_{r2}(t)$, and $\Omega_3(t) \equiv \sqrt{3}\,\Omega_{r3}(t)$. In what follows, the time-dependent quantities $\Omega_n(t)$ ($n = 1, 2, 3$), which differ from the original Rabi frequencies of external laser pulses only by constant prefactors, will also be referred to as Rabi frequencies. The structure of this last Hamiltonian, which is defined on a manifold of four states and has nonzero coupling only between adjacent ones, is illustrated in Fig. 2.

Importantly, one of the conditions of validity of the effective Hamiltonian in Eq. (4) is that $|V|T_{\text{int}} \gg 1$, where T_{int} is the relevant laser-pulse duration [37]. The last condition is equivalent to demanding that the interaction-induced energy shift $\hbar V$ is much larger than the Fourier-limited width of the laser pulses used, which precisely coincides with the definition of the Rydberg blockade regime. Thus, the above effective Hamiltonian is valid in the regime of primary interest for QIP with neutral atoms [54].

Generally speaking, Hamiltonians that are defined on a manifold of four states and have nonzero *real-valued* couplings only between adjacent states are characterized by the dynamical Lie algebra $su(2) \oplus su(2) \cong so(4)$ [this generalizes to analogous Hamiltonians defined on an n-state manifold, where the corresponding dynamical Lie algebra is $so(n)$]. Under the assumption of real-valued Rabi frequencies, this last dynamical symmetry was exploited in the context of W-to-GHZ state conversion in Ref. [37]. In what follows, we refrain from the restriction to real-valued Rabi frequencies and aim to determine the fastest possible (time-optimal) deterministic conversion between an initial W state and its GHZ counterpart.

Before embarking on the computation of the desired time-optimal W-to-GHZ state-conversion protocol, it is pertinent to make the following, symmetry-related remark. Namely, it is important to note that the states $|ggg\rangle$, $|W\rangle$, $|W'\rangle$, and $|rrr\rangle$ form an orthonormal basis of a four-dimensional subspace of the (eighth-dimensional) three-qubit Hilbert space $\mathcal{H} \equiv (\mathbb{C}^2)^{\otimes 3}$ that comprises the states invariant under an arbitrary permutation of qubits (i.e. invariant under the action of the symmetric group S_3); this four-dimensional subspace is usually referred to as the *symmetric sector* of the three-qubit

Hilbert space [55,56]. It is also worthwhile noting that for an arbitrary number of qubits — including the special case $N = 3$ of relevance here — both W- and GHZ states are invariant under an arbitrary permutation of qubits. Because both the initial- and final states of our envisioned W-to-GHZ state-conversion process belong to the symmetric sector, the fact that the effective system Hamiltonian in Eq. (4) involves the basis states of this particular subspace is pertinent from the symmetry standpoint.

III. QB APPROACH TO THE *W*-TO-GHZ STATE CONVERSION

In the following, we make use of the QB formalism [46] to determine the time-dependent Rabi frequencies $\Omega_n(t)$ ($n = 1, 2, 3$) that pertain to the time-optimal conversion of an initial W state $|\psi(t = 0)\rangle \equiv |W\rangle$ of the system at hand to the GHZ state $|\psi(t = T_{\text{QB}})\rangle \equiv (|ggg\rangle + e^{i\varphi}|rrr\rangle)/\sqrt{2}$. Here T_{QB} is the shortest possible state-conversion time, to be determined in what follows.

We first derive the QB equations pertaining to the time-optimal W-to-GHZ state conversion (Sec. III A). We then discuss the numerical scheme that we employ to determine the solution to these equations (Sec. III B).

A. Derivation of the QB equations for the time-optimal state conversion

We begin by representing the four three-qubit basis states $|ggg\rangle$, $|W\rangle$, $|W'\rangle$, and $|rrr\rangle$ by column vectors:

$$|ggg\rangle \mapsto \begin{pmatrix} 1 \\ 0 \\ 0 \\ 0 \end{pmatrix}, \quad |W\rangle \mapsto \begin{pmatrix} 0 \\ 1 \\ 0 \\ 0 \end{pmatrix},$$

$$|W'\rangle \mapsto \begin{pmatrix} 0 \\ 0 \\ 1 \\ 0 \end{pmatrix}, \quad |rrr\rangle \mapsto \begin{pmatrix} 0 \\ 0 \\ 0 \\ 1 \end{pmatrix}. \tag{5}$$

This allows us to express the effective system Hamiltonian $H(t)$ [cf. Eq. (4)] as

$$H(t) = \begin{pmatrix} 0 & \Omega_1(t) & 0 & 0 \\ \Omega_1^*(t) & 0 & \Omega_2(t) & 0 \\ 0 & \Omega_2^*(t) & 0 & \Omega_3(t) \\ 0 & 0 & \Omega_3^*(t) & 0 \end{pmatrix}, \tag{6}$$

where, for the sake of notational convenience, we set $\hbar = 1$ in the last equation; we will also keep this convention throughout the following derivation of the QB equations.

The original QB formalism [46] allows one to find the Hamiltonian $H(t)$ whose corresponding dynamics enable the shortest possible evolution of the system under consideration from a given initial- to a desired final state. That formalism is

based on a quantum action of the form

$$
\begin{aligned}
&S[H, |\psi\rangle, |\phi\rangle, \lambda] \\
&= \int dt \left[\frac{\sqrt{\langle\dot{\psi}|\dot{\psi}\rangle - |\langle\dot{\psi}|\psi\rangle|^2}}{\Delta E} \right. \\
&\left. + \sum_{j=1}^{M} \lambda_j f_j(H) + (i\langle\dot{\phi}|\psi\rangle + \langle\dot{\phi}|H|\psi\rangle + \text{c.c.}) \right].
\end{aligned}
\tag{7}
$$

Here $\Delta E \equiv \langle\psi|H^2|\psi\rangle - \langle\psi|H|\psi\rangle^2$ is the energy variance corresponding to the state $|\psi\rangle$ of the system and λ the shorthand for the set of M Lagrange multipliers λ_j ($j = 1, \ldots, M$); $|\phi\rangle$ is an auxiliary quantum state (a costate) that plays a role analogous to that of λ_j. A variation of H and $|\psi\rangle$ minimizes the Fubini-Study distance between the initial and final states, governed by the first term, and varying $|\phi\rangle$ in the third term ensures that $|\psi\rangle$ satisfies the Schrödinger equation. The second term gives rise to M additional, problem-specific constrains $f_j(H) = 0$ by varying the Lagrange multipliers λ_j.

While in the original QB formalism $\text{Tr}[H^2(t)]$ is fixed at any time [46], we weaken the latter restriction somewhat and fix only the total energy expended in the conversion process. In other words, the time-optimal state conversion is sought under the constraint of fixed total laser-pulse energy used, this last quantity being given by

$$
E = \int_0^T dt \sum_{n=1}^{3} |\Omega_n(t)|^2,
\tag{8}
$$

where T is the, as yet undetermined, total evolution time of the system. The last requirement is taken into account by imposing the constraint

$$
f_1(H) = \frac{1}{2} \text{Tr}\, H^2 - \frac{E}{T},
\tag{9}
$$

where $\text{Tr}\, H^2 = 2 \sum_{n=1}^{3} |\Omega_n|^2$, and choosing a constant Lagrange multiplier λ_1.

Moreover, we must ensure that the form of the Hamiltonian is preserved during the entire process. In other words, the time-dependent Hamiltonian of the system retains the form of Eq. (4) throughout the conversion process. This is ensured by imposing the constraint $\sum_{j=2}^{M} \lambda_j f_j(H) = \text{Tr}(\Lambda H)$, with

$$
\Lambda = \begin{pmatrix}
\lambda_{\text{gg}} & 0 & \lambda_{\text{gW'}} & \lambda_{\text{gr}} \\
0 & \lambda_{\text{WW}} & 0 & \lambda_{\text{Wr}} \\
\lambda_{\text{gW'}}^* & 0 & \lambda_{\text{W'W'}} & 0 \\
\lambda_{\text{gr}}^* & \lambda_{\text{Wr}}^* & 0 & \lambda_{\text{rr}}
\end{pmatrix},
\tag{10}
$$

where each Lagrange multiplier in Λ is time-dependent because $\text{Tr}(\Lambda H) = 0$ ought to hold at all times. General

constraints of this type have already been investigated in connection with quantum actions introduced in Ref. [46].

In line with Ref. [46], we perform the variation of all variables in Eq. (7) and arrive at the identities

$$
F = F|\psi\rangle\langle\psi| + |\psi\rangle\langle\psi|F - |\psi\rangle\langle\psi|\text{Tr}\, F,
\tag{11}
$$

$$
0 = (\dot{F} + i[H, F])|\psi\rangle,
\tag{12}
$$

where the operator F involves the constraint functions $f_j(H)$ and is given by

$$
F = \sum_{j=1}^{M} \lambda_j \partial_H f_j(H).
\tag{13}
$$

Due to the fact that λ_1 is a constant immaterial for our further discussion, we set $\lambda_1 = 1$, which further yields $F = H + \Lambda$. In particular, Eq. (12) implies that $F|\psi\rangle$ satisfies the Schrödinger equation, which leads to the equation of motion [48]

$$
\dot{F} = -i[H, F].
\tag{14}
$$

We first make use of Eq. (11) to derive the boundary values of F. By inserting $|\psi(0)\rangle$ and $|\psi(T)\rangle$ into this last equation, we readily obtain

$$
F(0) = \begin{pmatrix}
0 & \Omega_1(0) & 0 & 0 \\
\Omega_1^*(0) & \lambda_{\text{WW}}(0) & \Omega_2(0) & \lambda_{\text{Wr}}(0) \\
0 & \Omega_2^*(0) & 0 & 0 \\
0 & \lambda_{\text{Wr}}^*(0) & 0 & 0
\end{pmatrix},
$$

$$
F(T) = \begin{pmatrix}
\lambda_{\text{gg}}(T) & \Omega_1(T) & e^{-i\varphi}\Omega_3^*(T) & \lambda_{\text{gr}}(T) \\
\Omega_1^*(T) & 0 & 0 & e^{-i\varphi}\Omega_1^*(T) \\
e^{i\varphi}\Omega_3(T) & 0 & 0 & \Omega_3(T) \\
\lambda_{\text{gr}}^*(T) & e^{i\varphi}\Omega_1(T) & \Omega_3^*(T) & \lambda_{\text{rr}}(T)
\end{pmatrix}.
\tag{15}
$$

The next step is to bring the equation of motion in Eq. (14) to a more explicit form. By evaluating the diagonal elements of the matrix on the right-hand-side of this equation, one straightforwardly finds that these elements have the form of linear combinations $H_{jk}\Lambda_{jk}$, where either H_{jk} or Λ_{jk} is zero for each entry (j, k). This leads to the conclusion that the time derivatives of $\lambda_{\text{gg}}, \lambda_{\text{WW}}, \lambda_{\text{W'W'}}$, and λ_{rr}, which appear on the left-hand-side of Eq. (14) are equal to zero. Therefore, $\lambda_{\text{gg}}, \lambda_{\text{WW}}, \lambda_{\text{W'W'}}$, and λ_{rr} are constant. Moreover, by comparing $F(0)$ and $F(T)$ we conclude that $\lambda_{\text{gg}} = \lambda_{\text{WW}} = \lambda_{\text{W'W'}} = \lambda_{\text{rr}} = 0$. At the same time, $\text{Tr}\, F^n$ turns out to be constant for each $n \in \mathbb{N}$. In particular, by making use of the fact that $\text{Tr}\, F^3(0) = \text{Tr}\, F^3(T)$ we find that $\lambda_{\text{gr}}(T) = ie^{-i\varphi}|\lambda_{\text{gr}}(T)|$. On account of these last results, Eq. (14) leads to the following system of (nonlinear) ordinary differential equations (ODEs):

$$
\partial_t \begin{pmatrix}
0 & \Omega_1 & \lambda_{\text{gW'}} & \lambda_{\text{gr}} \\
\Omega_1^* & 0 & \Omega_2 & \lambda_{\text{Wr}} \\
\lambda_{\text{gW'}}^* & \Omega_2^* & 0 & \Omega_3 \\
\lambda_{\text{gr}}^* & \lambda_{\text{Wr}}^* & \Omega_3^* & 0
\end{pmatrix} = -i \begin{pmatrix}
0 & -\Omega_2^*\lambda_{\text{gW'}} & -\Omega_3^*\lambda_{\text{gr}} & \Omega_1\lambda_{\text{Wr}} - \Omega_3\lambda_{\text{gW'}} \\
\Omega_2\lambda_{\text{gW'}}^* & 0 & \Omega_1^*\lambda_{\text{gW'}} - \Omega_3^*\lambda_{\text{Wr}} & \Omega_1^*\lambda_{\text{gr}} \\
\Omega_3\lambda_{\text{gr}}^* & \Omega_3\lambda_{\text{Wr}}^* - \Omega_1\lambda_{\text{gW'}}^* & 0 & \Omega_2^*\lambda_{\text{Wr}} \\
\Omega_3^*\lambda_{\text{gW'}}^* - \Omega_1^*\lambda_{\text{Wr}}^* & -\Omega_1\lambda_{\text{gr}}^* & -\Omega_2\lambda_{\text{Wr}}^* & 0
\end{pmatrix}.
\tag{16}
$$

The next step amounts to noticing that it is possible to reduce the number of equations of motion by half by proving that the complex phases $\phi_1, \phi_2, \phi_3, \phi_{\mathrm{Wr}}, \phi_{\mathrm{gr}}, \phi_{\mathrm{gW'}}$ of the functions $\Omega_1, \Omega_2, \Omega_3, \lambda_{\mathrm{Wr}}, \lambda_{\mathrm{gr}}, \lambda_{\mathrm{gW'}}$ are constant in time. Assuming that those phases are time-independent, Eqs. (15) and (16) imply that the conditions

$$\phi_{\mathrm{Wr}} = -\phi_1 - \varphi, \quad \phi_{\mathrm{gW'}} = -\phi_3 - \varphi,$$
$$\phi_{\mathrm{gr}} = -\varphi - \frac{\pi}{2}, \quad \phi_2 = -\phi_1 - \phi_3 - \varphi - \frac{\pi}{2}, \quad (17)$$

ought to be satisfied; these restrictions imply that two out of three phases of the Rabi frequencies can be chosen arbitrarily (i.e., treated as free phases), while the third one is constrained by the chosen values of the first two. While the fulfillment of the conditions in Eq. (17), i.e., the assumption of time-independent complex phases leads to one solution of the system in Eq. (16) (for each fixed choice of initial values), the fact that the latter is a system of first-order equations guarantees the uniqueness of this solution. In other words, if the complex phases of each entry of $F(0)$ are consistent with the restrictions in Eq. (17), then F is uniquely determined by its initial value $F(0)$.

In the following, we consider ϕ_1 and ϕ_3 as free phases, while ϕ_2 is determined from Eq. (17) based on the values of ϕ_1 and ϕ_3. Given that the phases are found to be time-independent, we can reduce the problem at hand to finding the moduli of Ω_n and λ_k. The equation of motion in Eq. (16) then reduces to

$$\partial_t \begin{pmatrix} |\Omega_1| \\ |\Omega_2| \\ |\Omega_3| \\ |\lambda_{\mathrm{Wr}}| \\ |\lambda_{\mathrm{gr}}| \\ |\lambda_{\mathrm{gW'}}| \end{pmatrix} = \begin{pmatrix} -|\Omega_2||\lambda_{\mathrm{gW'}}| \\ |\Omega_1||\lambda_{\mathrm{gW'}}| - |\Omega_3||\lambda_{\mathrm{Wr}}| \\ |\Omega_2||\lambda_{\mathrm{Wr}}| \\ -|\Omega_1||\lambda_{\mathrm{gr}}| \\ |\Omega_1||\lambda_{\mathrm{Wr}}| - |\Omega_3||\lambda_{\mathrm{gW'}}| \\ |\Omega_3||\lambda_{\mathrm{gr}}| \end{pmatrix}. \quad (18)$$

Hence, we end up with the unknown initial values $|\Omega_1(0)|, |\Omega_2(0)|, |\lambda_{\mathrm{Wr}}(0)|$ and the unknown final values $|\Omega_1(T)|, |\Omega_3(T)|, |\lambda_{\mathrm{gr}}(T)|$. In addition, it is important to point out that the ODE system in Eq. (18) does not depend on the phase φ characterizing the GHZ state. This parameter can simply be determined by adjusting ϕ_2, based on the constraints in Eq. (17). Moreover, it is worthwhile to point out that the signs of the complex phases in Eq. (17) were chosen in such a way that the moduli in Eq. (18) remain positive during the entire state-conversion process.

Generally speaking, finding solutions of QB equations amounts to solving a two-point boundary value problem (BVP) in time. We now demonstrate that in this particular problem — finding the time-optimal W-to-GHZ state conversion in the system at hand — the relevant BVP can be reduced to the one that involves only two unknown initial values that are also bounded. To this end, we first derive an inequality to bound $|\Omega_1(0)|$ and $|\Omega_2(0)|$. From Eq. (18) it follows that

$$\frac{E}{T} = |\Omega_1|^2 + |\Omega_2|^2 + |\Omega_3|^2,$$
$$\frac{E_\Lambda}{T} = |\lambda_{\mathrm{gW'}}|^2 + |\lambda_{\mathrm{gr}}|^2 + |\lambda_{\mathrm{Wr}}|^2, \quad (19)$$

are both time-independent quantities. By evaluating both of these quantities at $t = 0$ and $t = T$, we obtain

$$\frac{E}{T} = |\Omega_1(0)|^2 + |\Omega_2(0)|^2,$$
$$\frac{E}{T} = |\Omega_1(T)|^2 + |\Omega_3(T)|^2,$$
$$\frac{E_\Lambda}{T} = |\lambda_{\mathrm{Wr}}(0)|^2,$$
$$\frac{E_\Lambda}{T} = |\lambda_{\mathrm{gW'}}(T)|^2 + |\lambda_{\mathrm{gr}}(T)|^2 + |\lambda_{\mathrm{Wr}}(T)|^2. \quad (20)$$

The constraints in Eq. (15) imply that $|\lambda_{\mathrm{Wr}}(T)| = |\Omega_1(T)|$ and $|\lambda_{\mathrm{gW'}}(T)| = |\Omega_3(T)|$, which, when inserted in Eq. (20), yields

$$\frac{E_\Lambda}{T} = |\lambda_{\mathrm{gr}}(T)|^2 + \frac{E}{T}. \quad (21)$$

The last equation leads to the conclusion that $E_\Lambda \geqslant E$ and, accordingly, $|\Omega_1(0)|^2 + |\Omega_2(0)|^2 \leqslant |\lambda_{\mathrm{Wr}}(0)|^2$.

The last conclusion enables us to bound the domain of the remaining initial values. To this end, we eliminate $|\lambda_{\mathrm{Wr}}(0)|$ by scaling the ODE system, given by Eq. (18). We also define

$$u_n = \frac{|\Omega_n|}{|\lambda_{\mathrm{Wr}}(0)|} \quad (n = 1, 2, 3),$$
$$w_k = \frac{|\lambda_k|}{|\lambda_{\mathrm{Wr}}(0)|} \quad (k = \mathrm{Wr, gr, gW'}), \quad (22)$$
$$\xi = |\lambda_{\mathrm{Wr}}(0)| t,$$

and the scaled (dimensionless) process time $\Xi = |\lambda_{\mathrm{Wr}}(0)|T$, such that the ODE system is invariant under the transformation $|\Omega_n| \mapsto u_n$, $|\lambda_k| \mapsto w_k$, and $t \mapsto \xi$. It should be kept in mind that the new variables ought to fulfill the initial conditions

$$u_3(0) = 0, \quad w_{\mathrm{gr}}(0) = 0, \quad w_{\mathrm{gW'}}(0) = 0, \quad (23)$$

as well as the final conditions

$$u_2(T) = 0, \quad w_{\mathrm{Wr}}(T) = u_1(T), \quad w_{\mathrm{gW'}}(T) = u_3(T), \quad (24)$$

which can be derived from Eq. (15).

Owing to the restriction $|\Omega_1(0)|^2 + |\Omega_2(0)|^2 \leqslant |\lambda_{\mathrm{Wr}}(0)|^2$, we know that the point $[u_1(0), u_2(0)]^{\mathrm{T}}$ lies within the unit circle, a bounded domain. It is thus pertinent to introduce polar coordinates (u, ϕ_u), in which $u_1(0) = u \cos \phi_u$, $u_2(0) = u \sin \phi_u$, and the following identity holds true:

$$u^2 = \frac{|\Omega_1(0)|^2 + |\Omega_2(0)|^2}{|\lambda_{\mathrm{Wr}}(0)|^2}. \quad (25)$$

In this manner, we have reduced the unknown initial values to the values of the polar radius u and the polar angle ϕ_u, which are both bounded, i.e.,

$$u \in [0, 1], \quad \phi_u \in [0, 2\pi]. \quad (26)$$

Using the column-vector representation of Eq. (5) we obtain the time-dependent Schrödinger equation

$$\partial_t \begin{pmatrix} \psi_{\mathrm{g}} \\ \psi_{\mathrm{W}} \\ \psi_{\mathrm{W'}} \\ \psi_{\mathrm{r}} \end{pmatrix} = -i \begin{pmatrix} \Omega_1 \psi_{\mathrm{W}} \\ \Omega_1^* \psi_{\mathrm{g}} + \Omega_2 \psi_{\mathrm{W'}} \\ \Omega_2^* \psi_{\mathrm{W}} + \Omega_3 \psi_{\mathrm{r}} \\ \Omega_3^* \psi_{\mathrm{W'}} \end{pmatrix}, \quad (27)$$

which governs the time evolution of the state

$$|\psi(t)\rangle = \psi_{\mathrm{g}}(t)|ggg\rangle + \psi_{\mathrm{W}}(t)|W\rangle$$
$$+ \psi_{\mathrm{W}'}(t)|W'\rangle + \psi_{\mathrm{r}}(t)|rrr\rangle \qquad (28)$$

of the system. Once again, we simplify the ODE system resulting from Eq. (27) by investigating, whether the phases $\phi_{\mathrm{g}}, \phi_{\mathrm{W}}, \phi_{\mathrm{W}'}, \phi_{\mathrm{r}}$ of the state components $\psi_{\mathrm{g}}, \psi_{\mathrm{W}}, \psi_{\mathrm{W}'}, \psi_{\mathrm{r}}$ are constant. The form of Eq. (27) bears out the assumption, if these phases satisfy the constraints

$$\phi_{\mathrm{g}} = \phi_{\mathrm{W}} + \phi_1 - \frac{\pi}{2},$$
$$\phi_{\mathrm{W}'} = \phi_{\mathrm{W}} + \phi_1 + \phi_3 + \varphi, \qquad (29)$$
$$\phi_{\mathrm{r}} = \phi_{\mathrm{W}} + \phi_1 + \varphi - \frac{\pi}{2},$$

where one of the phases can be chosen arbitrarily, e.g., ϕ_{W}. We emphasize that ϕ_{g} and ϕ_{r} only differ by φ, which is of crucial importance for generating the desired GHZ state.

By making use of the last conclusion about the phases of the state components ($\psi_{\mathrm{g}}, \psi_{\mathrm{W}}, \psi_{\mathrm{W}'}, \psi_{\mathrm{r}}$), and applying the transformation in Eq. (22), we can reduce the above time-dependent Schrödinger equation to an equation of motion that involves only the moduli of ($\psi_{\mathrm{g}}, \psi_{\mathrm{W}}, \psi_{\mathrm{W}'}, \psi_{\mathrm{r}}$):

$$\partial_\xi \begin{pmatrix} |\psi_{\mathrm{g}}| \\ |\psi_{\mathrm{W}}| \\ |\psi_{\mathrm{W}'}| \\ |\psi_{\mathrm{r}}| \end{pmatrix} = \begin{pmatrix} u_1|\psi_{\mathrm{W}}| \\ -u_1|\psi_{\mathrm{g}}| - u_2|\psi_{\mathrm{W}'}| \\ u_2|\psi_{\mathrm{W}}| - u_3|\psi_{\mathrm{r}}| \\ u_3|\psi_{\mathrm{W}'}| \end{pmatrix}. \qquad (30)$$

The boundary conditions inherent to the W-to-GHZ state-conversion problem under consideration are given by $|\psi_{\mathrm{W}}(0)| = 1$, $|\psi_{\mathrm{g}}(0)| = |\psi_{\mathrm{W}'}(0)| = |\psi_{\mathrm{r}}(0)| = 0$, $|\psi_{\mathrm{g}}(\Xi)| = |\psi_{\mathrm{r}}(\Xi)| = 1/\sqrt{2}$, and $|\psi_{\mathrm{W}}(\Xi)| = |\psi_{\mathrm{W}'}(\Xi)| = 0$. Once again, it should be stressed that φ only occurs in the restrictions of Eq. (29), whereas this phase does not appear in Eq. (30). Similar to what was done in Eq. (18) above, the signs of the complex phases in Eq. (29) are determined from the requirement that the moduli of the state components in Eq. (30) ought to remain positive during the process.

B. Numerical solution of the QB equations

As already pointed out above, finding solutions of QB equations amounts to solving a two-point BVP in time. Yet, this BVP is of a rather unconventional type as its final endpoint, which, e.g., in the problem at hand corresponds to the minimal state-conversion time, is unknown, being itself subject to minimization. While even standard two-point BVPs are far more demanding numerically than initial-value problems [53], this additional aspect of QB equations typically renders such equations rather difficult to solve numerically. This is the principal reason as to why only a handful of problems of this type have as yet been efficiently solved numerically and certain specialized approaches for the numerical treatment of QB equations have been proposed. For instance, in Ref. [49] an idea was proposed to treat QB paths as geodesics on the constraining manifold and determine the solutions of the QB equations by solving a set of geodesic equations. Another approach was proposed more

recently [57], which is based on a generalization of the original QB variational principle [46] and also makes use of the relaxation method [53] for solving the ensuing BVP.

In the problem under consideration, owing to the proposed parametrization of initial conditions by only two variables u and ϕ_u with bounded domains [cf. Eq. (26)], the relevant QB equations (i.e., the corresponding two-point BVPs) can efficiently be solved using the shooting method [53]. In other words, the character of the initial conditions in this problem obviates the need to use the aforementioned specialized numerical schemes. In line with the general idea of the shooting method, the initial values have to be chosen such that the functions occurring in the ODE system given by Eqs. (18) and (30) (Rabi frequencies, Lagrange multipliers, and state components) satisfy the corresponding final conditions at $\xi = \Xi$, where Ξ itself is as yet undetermined.

Within the framework of the shooting method, the initial conditions are modified iteratively in such a way that in the end the boundary conditions are fulfilled [53]. For each value of u and ϕ_u, the ODE system is solved within a certain time interval $[0, \xi_{\max}]$. Through a global minimization we determine the dimensionless time within this interval for which the functions in the ODE system have the smallest deviations from their imposed final conditions (cf. the Appendix). If the obtained smallest deviations vanish (i.e., if the functions do satisfy the final conditions) then the determined time is the sought-after minimal (dimensionless) state-conversion time Ξ_{QB}. If such time cannot be found within the interval $[0, \xi_{\max}]$ for any choice of u and ϕ_u then a successful state conversion is not possible and the upper bound $\xi_{\max}$ of the interval has to be increased. In other words, by varying the interval width $\xi_{\max}$ we can verify whether the smallest possible value for Ξ_{QB} was indeed obtained (for more details, see the Appendix).

It remains to clarify how to choose the starting points for the initial values. To avoid nonglobal minima in the aforementioned minimization of the deviation from the boundary conditions, it is necessary to check the entire domain of the initial values. In multidimensional problems, the shooting method can thus be a time- and resource-consuming approach [57]. However, here the domain of initial values is two-dimensional and bounded, which renders the problem at hand significantly simpler than in the generic case. As a result, we can perform the minimization starting from various initial values inside this domain with a moderate computational effort. This numerical computation, performed independently using three different minimization methods (for details, see the Appendix), yields the following values for u and ϕ_u: $(u, \phi_u) = (0.957, 0.311\pi)$ and $(u, \phi_u) = (0.957, 1.689\pi)$.

IV. RESULTS AND DISCUSSION

In the following, the principal findings of the present work, based on the numerical solution of the QB equations, are presented and discussed. In Sec. IV A we first present the central result of this article; the minimal state-conversion time T_{QB}. This is followed by the obtained results for the time-dependent Rabi frequencies that enable the time-optimal state conversion, and for the GHZ-state fidelity. To put the obtained results in perspective, in Sec. IV B we compare them with those found in the previously used dynamical-symmetry-based ap-
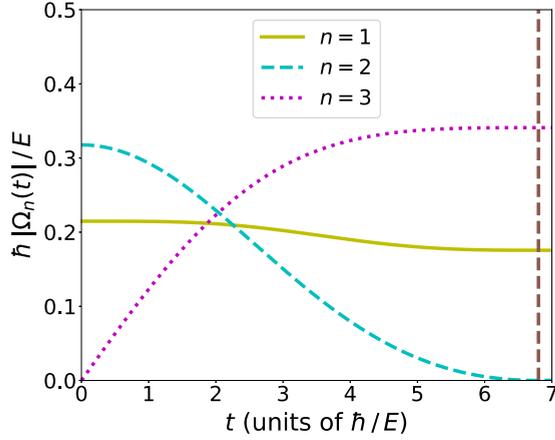
FIG. 3. Time evolution of the moduli of the complex-valued Rabi frequencies obtained numerically. The vertical dashed line marks the obtained minimal W-to-GHZ conversion time $T_{\mathrm{QB}} = 6.8\,\hbar/E$.

FIG. 4. Time dependence of the components $|\psi_\gamma(t)|$ of the state $|\psi(t)\rangle$ of the system obtained numerically. The vertical dashed line marks the obtained minimal W-to-GHZ conversion time $T_{\mathrm{QB}} = 6.8\,\hbar/E$.

proach. Finally, in Sec. IV C we demonstrate the robustness of the obtained time-optimal state-conversion scheme to deviations from the time-dependent Rabi frequencies found using the QB formalism.

A. Minimal state-conversion time and time dependence of Rabi frequencies

By inserting the obtained values for (u, ϕ_u) into the relevant ODE system [cf. Eqs. (18) and (30)] we obtain $\Xi_{\mathrm{QB}} = 2.72$ for the scaled state-conversion time in the time-optimal case. From this last value, it is straightforward to obtain the minimal state-conversion time T_{QB} in terms of the natural time scale $\hbar/E$ in the problem at hand (we reinstate $\hbar$ for this purpose).

We first recall that $|\lambda_{\mathrm{Wr}}(0)| = \sqrt{E_\Lambda/(\hbar T_{\mathrm{QB}})}$ and $\Xi_{\mathrm{QB}} = |\lambda_{\mathrm{Wr}}(0)|T_{\mathrm{QB}}$ [as follows from Eqs. (20) and (22), respectively], which immediately implies that $T_{\mathrm{QB}} = \hbar\,\Xi_{\mathrm{QB}}^2/E_\Lambda$. From Eqs. (20) and (25) it follows that $E = u^2 E_\Lambda$. By combining the last two expressions, we find that the minimal state-conversion time is given by

$$T_{\mathrm{QB}} = u^2\,\Xi_{\mathrm{QB}}^2\,\frac{\hbar}{E}. \tag{31}$$

By inserting the obtained numerical results for u and Ξ_{QB} into the last expression, we finally obtain $T_{\mathrm{QB}} = 6.8\,\hbar/E$, which represents the central result of this paper.

An equally important result of this paper pertains to the time dependence of the Rabi frequencies $\Omega_n(t) \equiv |\Omega_n(t)|e^{i\phi_n}$ that corresponds to the shortest possible state-conversion process. By making use of the solution $(u_0, \phi_{u0}) = (0.957, 0.311\pi)$ for the underlying BVP we obtain the time dependence of the moduli $|\Omega_n(t)|$ of these Rabi frequencies depicted in Fig. 3. It can easily be verified from this plot that the obtained results are consistent with the boundary conditions $|\Omega_3(0)| = 0$ and $|\Omega_2(T_{\mathrm{QB}})| = 0$. Another interesting feature of the obtained results is that $|\Omega_3(t)|$ reaches a constant finite value at $t = T_{\mathrm{QB}}$. The modulus $|\Omega_1(t)|$ of the third Rabi frequency does not vary appreciably during the process.
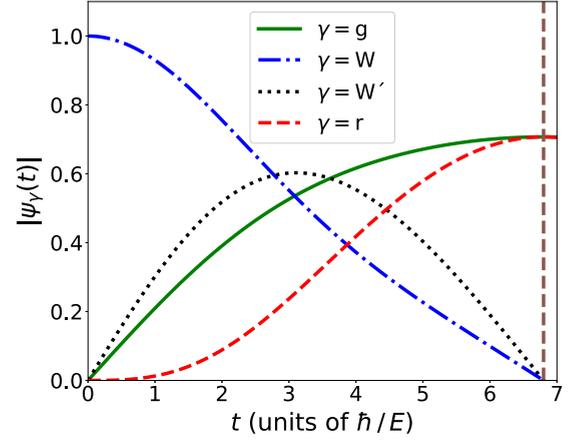
In view of the commonly occurring time-reversal-symmetric (or antisymmetric) solutions to quantum-control problems, it is pertinent to provide a comment as to why the Rabi frequencies in the problem at hand cannot be expected to display such behavior. Namely, this is apparent from Eq. (15), where $F(0) = \pm F(T)$ would lead to $|\Omega_2(0)| = |\lambda_{\mathrm{gr}}(0)| = |\lambda_{\mathrm{gW'}}(0)| = 0$, whereas Eq. (18) would imply that $|\Omega_2| = |\Omega_3| = |\lambda_{\mathrm{gW'}}| = 0$ are constant, which obviously does not constitute a solution of the problem at hand. Generally speaking, time-reversal-symmetric solutions for time-optimal processes are only expected if the initial and final state are related by a symmetry of the Hamiltonian [57].

While Fig. 3 only shows the moduli of the complex-valued time-dependent Rabi frequencies, it is pertinent to also comment at this point on their phases ϕ_1, ϕ_2, and ϕ_3. As concluded in Sec. III, these phases are constant (i.e., time-independent) and two out of three of them (e.g., ϕ_1 and ϕ_3) can take arbitrary values, while the remaining one is constrained by the chosen values of the first two [cf. Eq. (17)]. Both of these last two properties of the phases inherent to $\Omega_n(t)$ ($n = 1, 2, 3$) bode well for a potential experimental implementation of the laser pulses that correspond to the time-optimal state conversion.

The central figure of merit characterizing the envisioned W-to-GHZ state-conversion process is the GHZ-state fidelity $\mathcal{F}_{\mathrm{GHZ}}(t)$, which at time t is given by the modulus of the overlap of the target (GHZ) state and the actual state $|\psi(t)\rangle$ of the system at that time t [cf. Eq. (28)]. The time dependence of the four components $(\psi_{\mathrm{g}}, \psi_{\mathrm{W}}, \psi_{\mathrm{W'}}, \psi_{\mathrm{r}})$ of $|\psi(t)\rangle$ is illustrated in Fig. 4, which, among other things, correctly reflects the fact that at the very beginning of the state-conversion process ($t = 0$) we have that $|\psi_{\mathrm{W}}| = 1$, while at the end of this process ($t = T_{\mathrm{QB}}$) we have $|\psi_{\mathrm{g}}| = |\psi_{\mathrm{r}}| = 1/\sqrt{2}$.

Starting from the defining expression $\mathcal{F}_{\mathrm{GHZ}}(t) = |\langle \mathrm{GHZ}|\psi(t)\rangle|$, we straightforwardly find that the fidelity can be expressed as

$$\mathcal{F}_{\mathrm{GHZ}}(t) = \frac{1}{\sqrt{2}}|e^{i\phi_{\mathrm{g}}}|\psi_{\mathrm{g}}(t)| + e^{-i\varphi}e^{i\phi_{\mathrm{r}}}|\psi_{\mathrm{r}}(t)||. \tag{32}$$
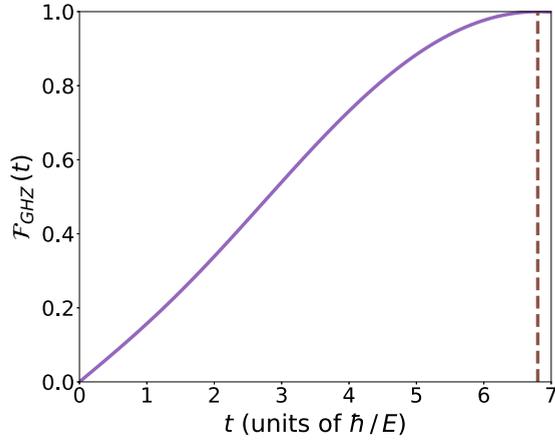
FIG. 5. Time dependence of the GHZ-state fidelity $\mathcal{F}_{\text{GHZ}}(t) = |\langle \text{GHZ}|\psi(t)\rangle|$ obtained numerically. The vertical dashed line marks the obtained minimal W-to-GHZ conversion time $T_{\text{QB}} = 6.8\,\hbar/E$ at which the fidelity reaches unity.

On account of the fact that $\phi_{\text{r}} \equiv \phi_{\text{g}} + \varphi$, as implied by Eq. (29), we finally obtain that

$$\mathcal{F}_{\text{GHZ}}(t) = \frac{|\psi_{\text{g}}(t)| + |\psi_{\text{r}}(t)|}{\sqrt{2}}. \qquad (33)$$

The GHZ-state fidelity—obtained numerically based on the last expression—is displayed in Fig. 5, from which it can be inferred that this fidelity shows monotonously increasing behavior and reaches unity at $t = T_{\text{QB}}$.

Importantly, the form of Eq. (33), which does not involve the phase φ characterizing the target GHZ state, allows us to draw an important conclusion. Namely, the GHZ-state fidelity in the problem at hand does not depend on φ at all. What makes this result plausible is the fact that only the phases ϕ_n of the complex-valued Rabi frequencies $\Omega_n(t)$ depend on φ, as can be inferred from the form of Eq. (17). Because these three phases are time-independent it is plausible that they lead to a φ-independent GHZ-state fidelity at an arbitrary time t during the state-conversion process ($0 \leqslant t \leqslant T_{\text{QB}}$). This also seems to be consistent with the fact that the entanglement-related properties of GHZ states (e.g., the fact that they have maximal essential three-way entanglement, as quantified by the 3-tangle [39]), also do not depend on φ.

B. Comparison to the dynamical-symmetry-based approach

The W-to-GHZ state-conversion problem in the Rydberg-atom system under consideration has recently been addressed using a dynamical-symmetry-based approach [37]. This approach allows one to carry out this conversion process up to five times faster than within the previously used shortcuts-to-adiabaticity approach [33]. It is thus pertinent to compare the state-conversion times T_{DS} found using that approach with the minimal time T_{QB} obtained here, where the comparison should be made under the assumption that the total laser-pulse energies used in both cases are the same.

Starting from the effective Hamiltonian in Eq. (4), the time dependence of the (real-valued) Rabi frequencies $\Omega_n(t)$ found

in Ref. [37] was shown to be given by

$$\Omega_n(t) = \frac{c_n}{T_{\text{DS}}(1 - \tau)} f\left(\frac{t}{T_{\text{DS}}}\right), \qquad (34)$$

where the function f is defined as

$$f(x) = \begin{cases} \frac{x}{\tau}, & 0 \leqslant x \leqslant \tau \\ 1, & \tau \leqslant x \leqslant 1 - \tau \\ \frac{1-x}{\tau}, & 1 - \tau \leqslant x \leqslant 1 \end{cases}, \qquad (35)$$

with $0 \leqslant \tau \leqslant 1/3$. This last time dependence corresponds to functions $|\Omega_n(t)|$ that grow from zero to a maximal value over the rise time $\tau\,T$, then remain constant during the time interval of the duration $T(1 - 2\tau)$, and, finally decay to zero during another interval of the duration $\tau\,T$. In the limiting case of vanishing rise/decay time ($\tau = 0$), the corresponding pulse has a rectangular shape.

By inserting the last functional form of $|\Omega_n(t)|$ into the expression for the total (fixed) laser-pulse energy [cf. Eq. (8)], we obtain

$$E = \hbar T_{\text{DS}} \sum_{n=1}^{3} \left|\frac{c_n}{T_{\text{DS}}(1 - \tau)}\right|^2 \int_0^1 dx\,|f(x)|^2. \qquad (36)$$

After a straightforward evaluation of the integral in the last equation, this finally leads to

$$E = \frac{\hbar}{T_{\text{DS}}} \sum_{n=1}^{3} |c_n|^2 \frac{3 - 4\tau}{3(1 - \tau)^2}. \qquad (37)$$

The coefficients $|c_n|$ in the last expression have the following values: $|c_1| = 1.225$, $|c_2| = 1.420$, and $|c_3| = 2.352$.

To be able to compare T_{DS} determined from Eq. (37) to the obtained minimal state-conversion time T_{QB}, it is sufficient to rearrange Eq. (37) in order to express T_{DS} in units of $\hbar/E$. In this manner, we find that $T_{\text{DS}}/T_{\text{QB}} = 1.66$ for $\tau = 1/3$ and $T_{\text{DS}}/T_{\text{QB}} = 1.33$ for $\tau = 0$. In other words, T_{QB} is in the range between $0.6\,T_{\text{DS}}$ (for $\tau = 1/3$) and $0.75\,T_{\text{DS}}$ (for $\tau = 0$). Thus, we arrive at the conclusion that the minimal state-conversion time T_{QB} is $25 - 40\%$ shorter than the state-conversion times previously found using the dynamical-symmetry-based approach. Given that T_{DS} is up to 5 times shorter than the state-conversion times obtained using shortcuts to adiabaticity [33], we can also conclude that the minimal state-conversion time T_{QB} is around 6.5 times shorter than the latter times.

Generally speaking, the capability of creating entanglement of a desired type on time scales significantly shorter than the coherence time of a quantum system is one of the prerequisites for QIP with that system. In particular, it has already been estimated that characteristic durations of W-to-GHZ state conversions using dynamical-symmetry-based approach are in the range $0.1 - 1\,\mu\text{s}$, which is $2 - 3$ orders of magnitude shorter than the typical radiative lifetimes of Rydberg states (around $100\,\mu\text{s}$ for a state with the principal quantum number $n_q \sim 50$ [58]). The minimal conversion times T_{QB} found here are even shorter, thus being significantly shorter than the relevant coherence times in Rydberg-atom systems.
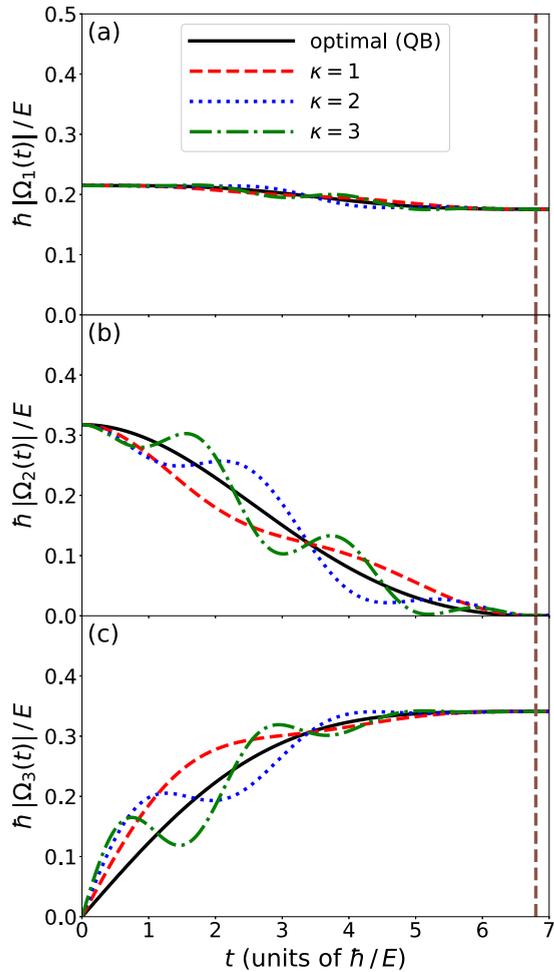
FIG. 6. Time dependence of the distorted Rabi frequencies [cf. Eq. (38)] for (a) $n = 1$, (b) $n = 2$, and (c) $n = 3$. The four curves for each value of n correspond to the optimal Rabi frequency and its three distorted counterparts (for $\kappa = 1, 2, 3$). The chosen value of the parameter t_n is equal to $0.1\,T_{QB}$. The vertical dashed line marks the obtained minimal W-to-GHZ conversion time $T_{QB} = 6.8\,\hbar/E$ at which the fidelity reaches unity.

FIG. 7. Deviation of the GHZ-state fidelity from unity (i.e., the infidelity), when Rabi frequency $|\Omega_n|$ is distorted ($n = 1, 2, 3$), at $t = T_{QB}$ for different values of the parameter t_n, shown for (a) $\kappa = 1$, (b) $\kappa = 2$, and (c) $\kappa = 3$.

C. Robustness of the state-conversion scheme against deviations from the optimal pulse shapes

Generally speaking, in applications where a high degree of control over the dynamics of quantum systems is required it is of interest to be able to quantify the error pertaining to deviations from optimal-control solutions of various problems [59–61]. In other words, it is often of paramount importance to be able to design control pulses which, while not being optimal, yield an error (compared to the optimal solution) not larger than some predefined threshold value and are, at the same time, more amenable to an experimental implementation.

In the W-to-GHZ state-conversion problem under consideration, using the QB formalism three time-dependent Rabi frequencies $\Omega_n(t)$ ($n = 1, 2, 3$) have been determined that lead to the time-optimal state conversion (cf. Fig. 3). In line with the above general considerations it is worthwhile to investigate the sensitivity of the state-conversion scheme at

hand, quantified by the GHZ-state fidelity $\mathcal{F}_{GHZ}$ at $t = T_{QB}$, with respect to deviations from the obtained optimal laser-pulse shapes. To this end, we consider the following form of (time-dependent) distortion from the optimal (QB) time dependence $\Omega_n(t)$ of the three Rabi frequencies [60]:

$$\delta|\Omega_n(t)| = t_n \sin\left(2\pi\kappa\frac{t}{T}\right)\frac{d}{dt}\,|\Omega_n(t)| \quad (n = 1, 2, 3). \quad (38)$$

Here κ is an integer-valued parameter that describes the rate of modulation of the optimal pulses, while the product of the prefactor t_n, which has units of time, and the first derivative of the Rabi frequency $\Omega_n(t)$ represents the amplitude of distortion for $\Omega_n(t)$ ($n = 1, 2, 3$). This last form of distortion is very general, as it is capable of reproducing, through an appropriate choice of the parameters t_n and κ, almost any realistic pulse shape.

The form of the distorted moduli $|\Omega_n(t)|$ of the time-dependent Rabi frequencies is illustrated in Fig. 6. The much less pronounced distortion of $|\Omega_1(t)|$ [Fig. 6(a)] compared to $|\Omega_2(t)|$ and $|\Omega_3(t)|$ [Figs. 6(b) and 6(c), respectively] can straightforwardly be understood based on the fact that the

original, time-optimal (i.e., obtained using the QB formalism) form of $|\Omega_1(t)|$ is characterized by a nearly time-independent behavior (cf. Fig. 3) and that the distortion in $|\Omega_n(t)|$ is, by design, proportional to its first derivative [cf. Eq. (38)].

The GHZ-state fidelity $\mathcal{F}_{\text{GHZ}}(t = T_{\text{QB}})$ corresponding to the distorted Rabi frequencies is straightforwardly obtained once the state $|\psi(t = T_{\text{QB}})\rangle$ of the system at $t = T_{\text{QB}}$ is determined. This is accomplished by propagating the time-dependent Schrödinger equation for the effective Hamiltonian of the system [cf. Eq. (4)] in a numerically exact fashion up to $t = T_{\text{QB}}$.

The obtained results for the deviation of the GHZ-state fidelity from unity at $t = T_{\text{QB}}$ [i.e., the infidelity $1 - \mathcal{F}_{\text{GHZ}}(t = T_{\text{QB}})$] as a result of distortion described by Eq. (38) are displayed for different values of t_n and κ in Fig. 7. What can be inferred from these results is that the reduction of the fidelity due to the assumed distortion of Rabi frequencies is quite small, being appreciable only for $\kappa = 1$ and extremely large values of t_n [cf. Fig. 7(a)]. The extremely large values of t_n, those close to T_{QB}, correspond to rather drastic distortions from the original time dependence of Rabi frequencies and are in fact not of practical relevance; realistic distortions are those corresponding to $t_n \lesssim T_{\text{QB}}/(2\pi\kappa)$, which for $\kappa = 1$ amounts to $t_n \lesssim 0.15\, T_{\text{QB}}$.

Therefore, through the numerical evaluation of the resulting target-state fidelities we have demonstrated that our time-optimal W-to-GHZ state-conversion scheme is extremely robust to possible deviations from the optimal shape of the relevant Rabi frequencies of external lasers. This bodes well for future experimental implementations of the proposed state-conversion scheme.

V. SUMMARY AND CONCLUSIONS

Using the quantum-brachistochrone formalism we have investigated the conversion of a W state into its GHZ counterpart in a system that consists of three gr-type Rydberg-atom qubits acted upon by four external laser pulses. Starting from an effective system Hamiltonian, we derived the quantum-brachistochrone equations describing the time-optimal dynamical evolution from the original W state to a GHZ state. We have solved numerically the underlying two-point boundary value problem using the shooting method and obtained the three time-dependent Rabi frequencies of external laser pulses that enable the desired, time-optimal state conversion. We have demonstrated that the minimal state-conversion time $T_{\text{QB}} = 6.8\,\hbar/E$, where E is the total laser-pulse energy used, is $25 - 40\%$ shorter than the state-conversion times recently obtained using a dynamical-symmetry-based approach with real-valued Rabi frequencies. In addition, we have also shown that the proposed time-optimal state-conversion is extremely robust to deviations from the optimal laser-pulse shapes.

Our work constitutes a highly nontrivial contribution to the growing body of work on quantum-state engineering in Rydberg-atom-based systems, one of the currently most promising platforms for large-scale quantum computing and analog quantum simulation. At the same time, the present work represents one of the very few examples to date of nontrivial quantum-control problems that have been fully solved within the quantum-brachistochrone framework. Our

approach—exploiting the form of the underlying equations to formulate a problem-specific parametrization of the initial conditions that drastically alleviates the computational burden that those equations entail–could possibly provide guidelines for solving other nontrivial time-optimality-related problems in the realm of quantum control.

The present work is likely to motivate future studies as it can be generalized not only to other state-conversion problems in the Rydberg-atom system considered here, but also to systems belonging to several other physical platforms for quantum computing. An experimental implementation of the time-optimal W-to-GHZ state-conversion protocol obtained here is clearly called for.

APPENDIX: DETAILS OF THE NUMERICAL IMPLEMENTATION

In the following, we provide the essential details of our numerical implementation of the shooting method for solving the two-point BVP of interest.

By making use of the proposed parametrization of initial conditions, we are now able to adjust the unknown initial values $\mathbf{x} \equiv (u, \phi_u)^{\text{T}}$, defined in Eq. (26), and the scaled evolution time Ξ with moderate computational effort. To guarantee that the final conditions of the variables $(u_1, u_2, u_3, w_{\text{Wr}}, w_{\text{gr}}, w_{\text{gW'}})$ in Eq. (24) and of the state components $(|\psi_{\text{g}}|, |\psi_{\text{W}}|, |\psi_{\text{W'}}|, |\psi_{\text{r}}|)$ are fulfilled, we list them in the vector

$$
d_{\mathbf{x}}(\xi) \equiv \begin{pmatrix} u_2(\xi) \\ u_1(\xi) - w_{\text{Wr}}(\xi) \\ u_3(\xi) - w_{\text{gW'}}(\xi) \\ |\psi_{\text{W}}(\xi)| \\ |\psi_{\text{W'}}(\xi)| \\ |\psi_{\text{g}}(\xi)| - |\psi_{\text{r}}(\xi)| \end{pmatrix}, \tag{A1}
$$

and minimize its Euclidean norm. To this end, it should be borne in mind that all functions appearing in the components of $d_{\mathbf{x}}(\xi)$ depend on the initial values $\mathbf{x}$.

In the numerical implementation, we fix an upper bound $\xi_{\max}$ of ξ. For given initial values $\mathbf{x}$, the ODE system in Eqs. (18) and (30) can straightforwardly be solved using the `odeint` solver from the `scipy.integrate` package [62] of the SciPy library. We define the error as

$$
D(\mathbf{x}) = \min_{\xi \in [0, \xi_{\max}]} \|d_{\mathbf{x}}(\xi)\|_2, \tag{A2}
$$

where $\|\mathbf{v}\|_2$ is the l_2-norm (i.e., Euclidean distance from the origin) of the vector $\mathbf{v}$. The scaled evolution time $\Xi(\mathbf{x}) \in [0, \xi_{\max}]$ is the time that corresponds to the minimum in Eq. (A2), i.e., $D(\mathbf{x}) = \|d_x(\Xi(\mathbf{x}))\|_2$. We minimize $D(\mathbf{x})$ with respect to $\mathbf{x}$ starting from $\mathbf{x}_0$.
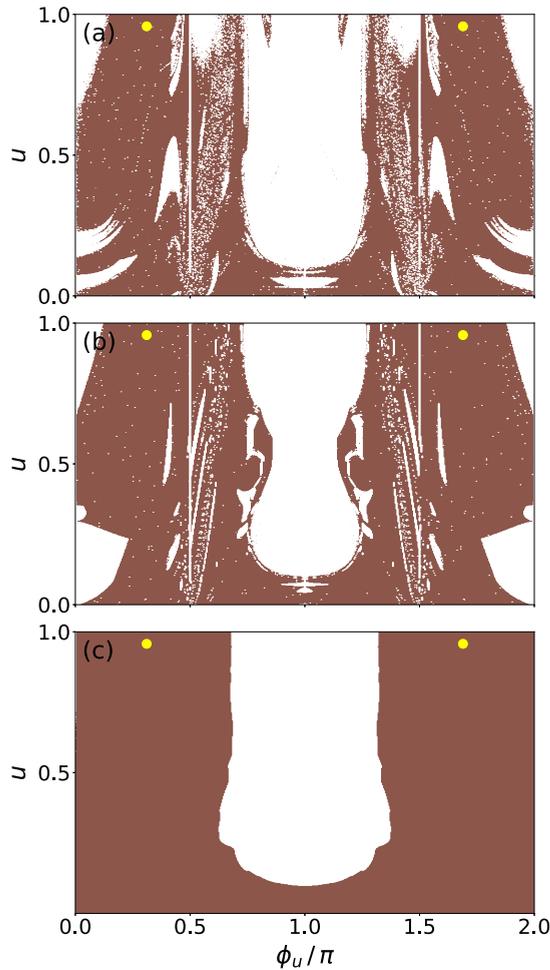
FIG. 8. Illustration of the minimization of $D(\mathbf{x})$ with initial values $\mathbf{x}_0 = (u_0, \phi_{u0})^\mathrm{T}$ using (a) the Newton method, (b) the BFGS algorithm, and (c) the Nelder-Mead method. In the dark and the white areas, respectively, the computation terminates with an error $D(\mathbf{x})$ smaller and greater than 0.1%. The two dots mark points $(u_0, \phi_{u0}) = (0.957, 0.311\pi)$ and $(u_0, \phi_{u0}) = (0.957, 1.689\pi)$, where the global minima are reached.

The minimization can be performed in several different ways. For instance, in Ref. [57] the Newton method was employed and the gradient of the function to be minimized was computed numerically. In keeping with this procedure, we compute the gradient of $D(\mathbf{x})$ by evaluating the derivatives of $\boldsymbol{d}_\mathbf{x}(\Xi(\mathbf{x}))$ according to

$$
\begin{aligned}
\partial_j D(\mathbf{x}) &= \frac{\boldsymbol{d}_x(\Xi(\mathbf{x})) \cdot \partial_j \boldsymbol{d}_\mathbf{x}(\Xi(\mathbf{x}))}{\|\boldsymbol{d}_\mathbf{x}(\Xi(\mathbf{x}))\|_2}, \\
\partial_j \boldsymbol{d}_\mathbf{x}(\Xi(\mathbf{x})) &= \frac{\boldsymbol{d}_{\mathbf{x}+\epsilon \boldsymbol{e}_j}(\Xi(\mathbf{x}+\epsilon \boldsymbol{e}_j)) - \boldsymbol{d}_\mathbf{x}(\Xi(\mathbf{x}))}{\epsilon},
\end{aligned}
\tag{A3}
$$
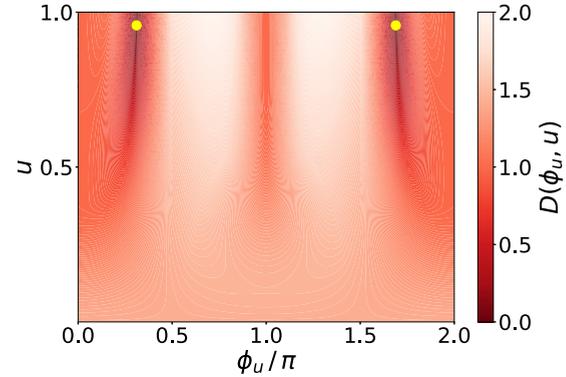
FIG. 9. The error $D(\mathbf{x}) \equiv D(u, \phi_u)$ for initial values (u, ϕ_u) without minimization with respect to $\mathbf{x}$. The two dots mark points $(u_0, \phi_{u0}) = (0.957, 0.311\pi)$ and $(u_0, \phi_{u0}) = (0.957, 1.689\pi)$, where the global minima are reached.

with ∂_j ($j = 1, 2$) being a shorthand for the partial derivative ∂/∂_{x_j}, where $x_1 \equiv u$ and $x_2 \equiv \phi_u$; $\boldsymbol{e}_j$ denote the corresponding unit vectors. It is important to stress that accurate numerical evaluation of the derivatives in the last equation requires ϵ to be sufficiently small and the value $\epsilon = 10^{-6}$ was used in the actual evaluation. It is also worthwhile mentioning that we adjust Ξ in the course of our numerical procedure, in contrast to Ref. [57] where $\mathbf{x}$ is computed for fixed Ξ.

In addition to the Newton method, we solved the same problem independently using the Broyden-Fletcher-Goldfarb-Shanoo algorithm and the Nelder-Mead method [53]. We investigated various initial values $u_0 = n_s/N$ and $\phi_{u0} = 2\pi n_s/N$, where $n_s = 0 \dots N$ and $N = 500$ was chosen. Figure 8 shows the areas in which a global minimum is found, that is, the error $D(\mathbf{x})$ drops below 0.1%. In these areas, the numerical computation terminates successfully at $(u_0, \phi_{u0}) = (0.957, 0.311\pi)$ and $(u_0, \phi_{u0}) = (0.957, 1.689\pi)$, where $\Xi = 2.72$ and $D(\mathbf{x}_0) = 0.03\%$. Hence, all three minimization methods return the same values for global minima. For the sake of completeness, the error $D(\mathbf{x})$ itself (without minimization over $\mathbf{x}$) is displayed in Fig. 9.

To verify that $T_{\mathrm{QB}} = 6.8 \, \hbar/E$ indeed represents the shortest possible state-conversion time, we perform numerical evaluation for different upper bounds $\xi_{\max}$. Since $\mathbf{x}_0$ might vary, we compute the global minimum $\min_\mathbf{x} D(\mathbf{x})$ of the error $D(\mathbf{x})$ for each $\tau_{\max}$ using different minimization methods. The corresponding state-conversion time T turns out to be as large as possible for $\xi_{\max} < 2.72$ and stays constant for $\xi_{\max} \geqslant 2.72$. Along with the observation that our calculations consistently show a strictly positive error until $T = T_{\mathrm{QB}} = 6.8 \, \hbar/E$ is reached, this constitutes the evidence that $6.8 \, \hbar/E$ is the minimal state-conversion time.

[1] J. P. Dowling and G. J. Milburn, Philos. Trans. R. Soc. A **361**, 1655 (2003).

[2] W. Dür, G. Vidal, and J. I. Cirac, Phys. Rev. A **62**, 062314 (2000).

[3] D. M. Greenberger, M. A. Horne, and A. Zeilinger, in *Bell's Theorem, Quantum Theory, and Conceptions of the Universe* (Kluwer Academic, Dordrecht, 1989), pp. 73–76.

[4] M. A. Nielsen and I. L. Chuang, *Quantum Computation and Quantum Information* (Cambridge University Press, Cambridge, 2000).

[5] J. Joo, Y.-J. Park, S. Oh, and J. Kim, New J. Phys. **5**, 136 (2003).

[6] C. Zhu, F. Xu, and C. Pei, Sci. Rep. **5**, 17449 (2015).

[7] C. Li and Z. Song, Phys. Rev. A **91**, 062104 (2015).

[8] Y.-H. Kang, Y.-H. Chen, Z.-C. Shi, J. Song, and Y. Xia, Phys. Rev. A **94**, 052311 (2016).

[9] Y.-H. Kang, Y.-H. Chen, Q.-C. Wu, B.-H. Huang, J. Song, and Y. Xia, Sci. Rep. **6**, 36737 (2016).

[10] V. M. Stojanović, Phys. Rev. Lett. **124**, 190504 (2020).

[11] J. Peng, J. Zheng, J. Yu, P. Tang, G. A. Barrios, J. Zhong, E. Solano, F. Albarrán-Arriagada, and L. Lamata, Phys. Rev. Lett. **127**, 043604 (2021).

[12] V. M. Stojanović, Phys. Rev. A **103**, 022410 (2021).

[13] J. Zheng, J. Peng, P. Tang, F. Li, and N. Tan, Phys. Rev. A **105**, 062408 (2022).

[14] T. Haase, G. Alber, and V. M. Stojanović, Phys. Rev. Research **4**, 033087 (2022).

[15] G.-Q. Zhang, W. Feng, W. Xiong, Q.-P. Su, and C.-P. Yang, arXiv:2205.13920.

[16] A. S. Coelho, F. A. S. Barbosa, K. N. Cassemiro, A. S. Villar, M. Martinelli, and P. Nussenzveig, Science **326**, 823 (2009).

[17] C. Song, K. Xu, W. Liu, C.-P. Yang, S.-B. Zheng, H. Deng, Q. Xie, K. Huang, Q. Guo, L. Zhang *et al.*, Phys. Rev. Lett. **119**, 180511 (2017).

[18] M. Erhard, M. Malik, M. Krenn, and A. Zeilinger, Nat. Photonics **12**, 759 (2018).

[19] V. Macrì, F. Nori, and A. F. Kockum, Phys. Rev. A **98**, 062327 (2018).

[20] I. Dhand, M. Engelkemeier, L. Sansoni, S. Barkhofen, C. Silberhorn, and M. B. Plenio, Phys. Rev. Lett. **120**, 130501 (2018).

[21] R.-H. Zheng, Y.-H. Kang, Z.-C. Shi, and Y. Xia, Ann. Phys. (Berlin) **531**, 1800447 (2019).

[22] J. Nogueira, P. A. Oliveira, F. M. Souza, and L. Sanz, Phys. Rev. A **103**, 032438 (2021).

[23] E. Pachniak and S. A. Malinovskaya, Sci. Rep. **11**, 12980 (2021).

[24] Y.-F. Qiao, J.-Q. Chen, X.-L. Dong, B.-L. Wang, X.-L. Hei, C.-P. Shen, Y. Zhou, and P.-B. Li, Phys. Rev. A **105**, 032415 (2022).

[25] M. Saffman, J. Phys. B **49**, 202001 (2016).

[26] For a recent review, see L. Henriet, L. Beguin, A. Signoles, T. Lahaye, A. Browaeys, G.-O. Reymond, and C. Jurczak, Quantum **4**, 327 (2020).

[27] For an extensive review, see, e.g., M. Morgado and S. Whitlock, AVS Quantum Sci. **3**, 023501 (2021).

[28] For an up-to-date review, see X.-F. Shi, Quantum Sci. Technol. **7**, 023002 (2022).

[29] L. F. Buchmann, K. Mølmer, and D. Petrosyan, Phys. Rev. A **95**, 013403 (2017).

[30] M. Ostmann, J. Minář, M. Marcuzzi, E. Levi, and I. Lesanovsky, New J. Phys. **19**, 123015 (2017).

[31] S. A. Malinovskaya, Opt. Lett. **42**, 314 (2017).

[32] A. Omran, H. Levine, A. Keesling, G. Semeghini, T. T. Wang, S. Ebadi, H. Bernien, A. S. Zibrov, H. Pichler, S. Choi *et al.*, Science **365**, 570 (2019).

[33] R.-H. Zheng, Y.-H. Kang, D. Ran, Z.-C. Shi, and Y. Xia, Phys. Rev. A **101**, 012345 (2020).

[34] T. M. Wintermantel, Y. Wang, G. Lochead, S. Shevate, G. K. Brennen, and S. Whitlock, Phys. Rev. Lett. **124**, 070503 (2020).

[35] R. Mukherjee, H. Xie, and F. Mintert, Phys. Rev. Lett. **125**, 203603 (2020).

[36] X.-F. Shi, Phys. Rev. Applied **13**, 024008 (2020).

[37] T. Haase, G. Alber, and V. M. Stojanović, Phys. Rev. A **103**, 032427 (2021).

[38] D. Zhu, G.-G. He, and F.-L. Zhang, Phys. Rev. A **105**, 062202 (2022).

[39] V. Coffman, J. Kundu, and W. K. Wootters, Phys. Rev. A **61**, 052306 (2000).

[40] R. Horodecki, P. Horodecki, M. Horodecki, and K. Horodecki, Rev. Mod. Phys. **81**, 865 (2009).

[41] P. Walther, K. J. Resch, and A. Zeilinger, Phys. Rev. Lett. **94**, 240501 (2005).

[42] W. X. Cui, S. Hu, H. F. Wang, A. D. Zhu, and S. Zhang, Opt. Express **24**, 15319 (2016).

[43] Y. H. Kang, Z. C. Shi, B. H. Huang, J. Song, and Y. Xia, Phys. Rev. A **100**, 012332 (2019).

[44] J. Song, X. D. Sun, Q. X. Mu, L. L. Zhang, Y. Xia, and H. S. Song, Phys. Rev. A **88**, 024305 (2013).

[45] G. Y. Wang, D. Y. Wang, W. X. Cui, H. F. Wang, A. D. Zhu, and S. Zhang, J. Phys. B **49**, 065501 (2016).

[46] A. Carlini, A. Hosoya, T. Koike, and Y. Okudaira, Phys. Rev. Lett. **96**, 060503 (2006).

[47] L. Haws and T. Kiser, Am. Math. Mon. **102**, 328 (1995).

[48] A. Carlini, A. Hosoya, T. Koike, and Y. Okudaira, Phys. Rev. A **75**, 042308 (2007).

[49] X. Wang, M. Allegra, K. Jacobs, S. Lloyd, C. Lupo, and M. Mohseni, Phys. Rev. Lett. **114**, 170501 (2015).

[50] T. Caneva, M. Murphy, T. Calarco, R. Fazio, S. Montangero, V. Giovannetti, and G. E. Santoro, Phys. Rev. Lett. **103**, 240501 (2009).

[51] A. del Campo, I. L. Egusquiza, M. B. Plenio, and S. F. Huelga, Phys. Rev. Lett. **110**, 050403 (2013).

[52] M. R. Lam, N. Peter, T. Groh, W. Alt, C. Robens, D. Meschede, A. Negretti, S. Montangero, T. Calarco, and A. Alberti, Phys. Rev. X **11**, 011035 (2021).

[53] W. H. Press, S. A. Teukolsky, W. T. Vetterling, and B. P. Flannery, *Numerical Recipes in C: The Art of Scientific Computing* (Cambridge University Press, Cambridge, 1999).

[54] X.-F. Shi, Phys. Rev. Applied **9**, 051001(R) (2018).

[55] P. Ribeiro and R. Mosseri, Phys. Rev. Lett. **106**, 180502 (2011).

[56] F. Albertini and D. D'Alessandro, J. Math. Phys. **59**, 052102 (2018).

[57] D. Wang, H. Shi, and Y. Lan, New J. Phys. **23**, 083043 (2021).

[58] T. F. Gallagher, *Rydberg Atoms* (Cambridge University Press, Cambridge, 1994).

[59] T.-S. Ho, J. Dominy, and H. Rabitz, Phys. Rev. A **79**, 013422 (2009).

[60] See, e.g., A. Negretti, R. Fazio, and T. Calarco, J. Phys. B **44**, 154012 (2011).

[61] See, e.g., V. M. Stojanović, Phys. Rev. A **99**, 012345 (2019).

[62] The reference material is given at the following URL: https://docs.scipy.org/doc/scipy/reference/generated/scipy.integrate.odeint.html.